Biochimica et Biophysica Acta 1798 (2010) 928–937

Contents lists available at ScienceDirect

Biochimica et Biophysica Acta

journal homepage: www.elsevier.com/locate/bbamem

Effect of monolayer lipid charges on the structure and orientation of protein VAMP1 at the air–water interface

Wissam Yassine, Alexandra Milochau, Sebastien Buchoux, Jochen Lang, Bernard Desbat [1], Reiko Oda *,[1]

Université de Bordeaux, UMR CBMN 5248, CNRS, Institut Européen de Chimie et Biologie, 2, rue Robert Escarpit, F-33607 PESSAC, France

ARTICLE INFO

Article history:
Received 26 August 2009
Received in revised form 2 December 2009
Accepted 13 January 2010
Available online 18 January 2010

Keywords:
SNARE protein
Synaptobrevin
PMIRRAS
Brewster angle microscope
Protein–lipid interaction

ABSTRACT

SNARE proteins are implicated in membrane fusion during neurotransmission and peptide hormone secretion. Relatively little is known about the molecular interactions of their trans- and juxtamembrane domains with lipid membranes. Here, we report the structure and the assembling behavior of one of the SNARE proteins, VAMP1/synaptobrevin1 incorporated in a lipid monolayer at an air–water interface which mimics the membrane environment. Our results show that the protein is extremely sensitive to surface pressure as well as the lipid composition. Monolayers of proteins alone or in the presence of the neutral phospholipid DMPC underwent structural transition from α-helix to β-sheet upon surface compression. In contrast, the anionic phospholipid DMPG inhibited this transition in a concentration-dependent manner. Moreover, the orientation of the proteins was highly sensitive to the charge density of the lipid layers. Thus, the structure of VAMP1 is clearly controlled by protein–lipid interactions.

1. Introduction

A set of evolutionary conserved membrane proteins plays a major role within cells during the fusion of proteolipid membranes, a process that forms the base of events such as neurotransmission, hormone secretion, intracellular vesicular transport or membrane repair [1]. The crystal structure of the cytosolic core complex has been resolved [2,3]. The single-span integral membrane proteins VAMP/synaptobrevin, residing in vesicle membranes, and syntaxin 1 in the plasma membrane, as well as the peripheral plasma membrane protein SNAP25 form a stable ternary "trans-complex" through their cytosolic domains thus bridging the two membranes. The membrane fusion requires the interaction of the cytosolic domains of the SNARE proteins which constitutes a minimal membrane fusion machinery [4–6].

In contrast, the configuration of the transmembrane domains has only recently been addressed due to the inherent difficulties in determining membrane-embedded structures. Previously, we have investigated the structure and orientation of the non-modified transmembrane domain of the SNARE protein VAMP1 in various lipid environments using synthetic peptides. This study revealed an unprecedented dynamic and reversible switch between α-helical and β-sheet structure of the peptides depending on the peptide to lipid ratio and the nature of the lipids [7].

We now investigated the assembling behavior and the structure of full-length recombinant VAMP1 at the air–water interface. Using Brewster angle microscopy (BAM) and polarization modulation-infrared reflection-adsorption spectroscopy (PMIRRAS), we addressed the presence of molecular aggregates at a macroscopic level as well as the molecular structures in these aggregates. Experiments were performed in the presence of neutral and negatively charged lipids in order to address the protein–protein and protein–lipid interactions, in particular the potential influence of the juxtamembrane and cytoplasm fragments of the full-length protein on the organization of the transmembrane fragment.

Our results indicate that the structure and orientation of VAMP spread at air/water interface was highly sensitive to the lipid environment and the surface pressure. The BAM images of monolayers of VAMP deposited alone or mixed with zwitterionic phospholipids DMPC exhibited domain segregation upon compression. This probably reflects the instalment of protein-rich and protein-depleted domains upon compression accompanied by reversible structural transition from α-helix to β-sheet as observed by PMIRRAS. In contrast, the presence of anionic phospholipids DMPG above a certain concentration rendered the monolayers more homogeneous and the structure of the proteins remained α-helical even at a high surface pressure. The orientation of the α-helices in regard to the interface depends largely on the surface charge density of the lipid monolayer. Thus, the interaction between the lipid charge and the juxtamembrane domain of the proteins clearly plays an important role in determining the protein structure.

* Corresponding author. Postal address: R. Oda, IECB, 2, av Robert Escarpit, 33607 PESSAC-CEDEX, France.
E-mail addresses: b.desbat@cbmn.u-bordeaux.fr (B. Desbat), r.oda@iecb.u-bordeaux.fr (R. Oda).
[1] Both authors contributed equally.

0005-2736/$ – see front matter © 2010 Elsevier B.V. All rights reserved.
doi:10.1016/j.bbamem.2010.01.009

2. Materials and methods

2.1. Lipids and proteins

1,2-Dimyristoyl-*sn*-glycero-3-phophatidylcholine (DMPC) and 1,2-dimyristoyl-*sn*-glycero-3-[phospho-*rac*-(1-glycerol)] (sodium salt) (DMPG) with a purity <99% were purchased from Sigma-Aldrich. Water (resistivity: 18.2 MΩ) used for buffer preparation was filtered and deionized with an ELGA apparatus. Recombinant GST-VAMP1 (rat) was expressed in *E. coli* BL21, solubilized in Triton-X100 containing buffer and bound to glutathione beads [8,9]. After exchanging the detergent for 0.8% octylglucoside, VAMP was eluted from the beads by thrombin cleavage, concentrated and further purified by FPLC (Superdex75). Purified proteins were stored at −80 in phosphate-buffered saline containing 0.8% octylglucoside and 10% glycerol. The sequence of VAMP1 is MSAPAQPPAE GTEGAAPGGG PPGPPPNTTS NRRLQQTQAQ VEEVVDIIRV NVDKVLERDQ LSELDDRAD ALQAGASVFE SSAAKLKRKY WWKNCK*MMIM LGAICAIIVV VIVIYIFT* with 96 amino acids in the cytosolic domain (12 positive charges, 13 negative charges, 25 polar neutral, and 46 non polar at pH 7.4) and 22 amino acids in the transmembrane domain.

2.2. Film formation and surface pressure measurements

Monolayer experiments were performed on a computer-controlled Langmuir film balance (Nima Technology, Coventry, UK). The rectangular trough ($V = 150\ cm^3$, $S = 300\ cm^2$) and the barrier were made of Teflon. Phospholipids were dissolved in chloroform (DMPC) or chloroform/methanol (DMPG, DMPC/DMPG). First, the trough was filled with a phosphate buffer (130 mM KCl, 5 mM NaCl, 13 mM Na_2HPO_4, 10 mM $MgSO_4$, pH 7.4). A solution of protein molecules was deposited onto the subphase surface using a calibrated Hamilton microsyringe. Thirty minutes after incubation, a protein monolayer compression/decompression cycle at the surface was exerted to ensure a homogenous repartition of the VAMP1 at the top of the subphase. Subsequently phospholipids were injected on the decompressed protein layer in order to form a mixed layer of protein/phospholipids. The quantities of spread protein and protein/phospholipid ratios were controlled such that protein/lipid films with about 1/33 and 1/83 molar fractions were obtained at 0 mN/m surface pressure before film compression. Note that after injection of VAMP1 at the buffer interface, about 40% of the protein went from the interface into the subphase. The values presented in this manuscript are those present after the calibration, i.e. in order to obtain the 1/33 or 1/83 protein/lipid films, 1 protein molecule per 20 or 50 lipid molecules were injected.

Surface pressure (π) was measured by the Wilhelmy method using a filter paper plate. Compression–expansion cycles were performed at a rate of 10 cm^2/min and isotherms were displayed by plotting the surface pressure versus area per phospholipid molecule.

2.3. Brewster angle microscopy (BAM)

The morphology of protein and protein/lipid monolayers at the air–water interface was observed using a Brewster angle microscope (NFT BAM*2plus*, Göttingen, Germany) [10] mounted on a computer-controlled Teflon Langmuir film balance (300 cm^2) (Nima Technology, Coventry, UK). The microscope was equipped with a frequency doubled Nd:Yag laser (532 nm; 50 mW), polarizer, analyzer and CCD camera. The exposition time (ET) depends on the shutter speed. The spatial resolution of the BAM was about 2 μm and the image size was 600×450 μm. The reflectivity calibration obtained from the grey level and the layer thickness estimate, (using the refractive index of water $n = 1.33$ and of the protein monolayer $n = 1.47$ (for pure lipids, $n = 1.46$)) were calculated with the BAM*2plus* software package (I-Elli2000) [11,12].

2.4. PMIRRAS spectroscopy

Monolayers at the air–buffer interface were monitored in situ by PMIRRAS [13]. PMIRRAS spectra were recorded during monolayer compression–expansion on a Nicolet 870 spectrometer equipped with a photovoltaic HgCdTe detector cooled at 77 K [14]. Generally 600 scans were co-added at a resolution of 8 cm^{-1} for pure protein and mixed protein/lipid (DMPC, DMPG, DMPC/DMPG) monolayers. The PMIRRAS spectrometer was set up as follows: an IR beam was polarized by a ZnSe polarizer and modulated by a ZnSe photoelastic modulator between parallel (p) and perpendicular (s) polarizations to the incidence plane. The two channel processing of the detected signal gives the differential reflectivity spectrum $\Delta R/R = (R_p - R_s)/(R_p + R_s)$ where R_p and R_s are the polarized reflectivities. To remove the contribution of liquid water absorption, each IR spectrum is divided by the corresponding spectrum of the subphase. PMIRRAS intensity is a function of the number of molecules per unit surface and a function of the molecular conformation and orientation. During compression the number of molecules per area unit increases, increasing the infrared absorption. Mao et al. have shown [15] that the PMIRRAS signal is proportional to two parameters: the number of molecules per unit area and an orientation function f(θ):

$$I_{PM-IRRAS} \propto \frac{N}{A} \cdot f(\theta)$$

where I is the intensity of the normalized PMIRRAS signal, N is the number of molecules on the surface, A is the area of the trough at a given pressure and θ is the average tilt angle of the transition moment with respect to the normal surface. When the number of molecules is kept constant during the experiment, the product $I \cdot A$ is directly proportional to the orientation function f(θ):

$$f(\theta) = \sin^2\theta - \sin^2\theta_m$$

θ_m is the magic angle of PMIRRAS on water ($\theta_m = 38°$), when $\theta = \theta_m$ the adsorption disappears.

The differential reflectivity measurement allows us to follow orientation and secondary structure changes at the interface.

3. Results

VAMP1 is amphiphilic as it contains 22 amino acids in the hydrophobic transmembrane domain and 98 amino acids in its soluble cytosolic portion. When deposited at air–water interface, the protein remains therefore at the interface to form a monolayer. This characteristic allows studying their aggregation behavior and their structure by the Brewster angle microscope and PMIRRAS, respectively, in the presence or absence of lipids.

3.1. VAMP1 as protein monolayer

A Langmuir trough was filled with a solution of phosphate buffer and indicated quantities of VAMP1 in PBS (containing octyl-n-glucoside, pH 7.4) were injected onto the subphase. Fig. 1 depicts the isotherm curves of surface pressure during compression and decompression (Fig. 1E) along with BAM images (Fig. 1A–D) and PMIRRAS spectra (Fig. 1F) taken at various surface pressures. Subsequent to the injection of VAMP1 at the air–water interface, the luminosity of the interface seen from BAM images (Fig. 1A) increased slightly and homogeneously with just a few bright spots representing probably small protein aggregates. The surface pressure remained at 0 mN/m, which indicated that the proteins adsorb to the surface and that only few protein–protein interactions occurred at this surface concentration. The average layer thickness was 0.7 nm as calculated from the BAM luminosity (grey levels) using a refractive index of 1.47

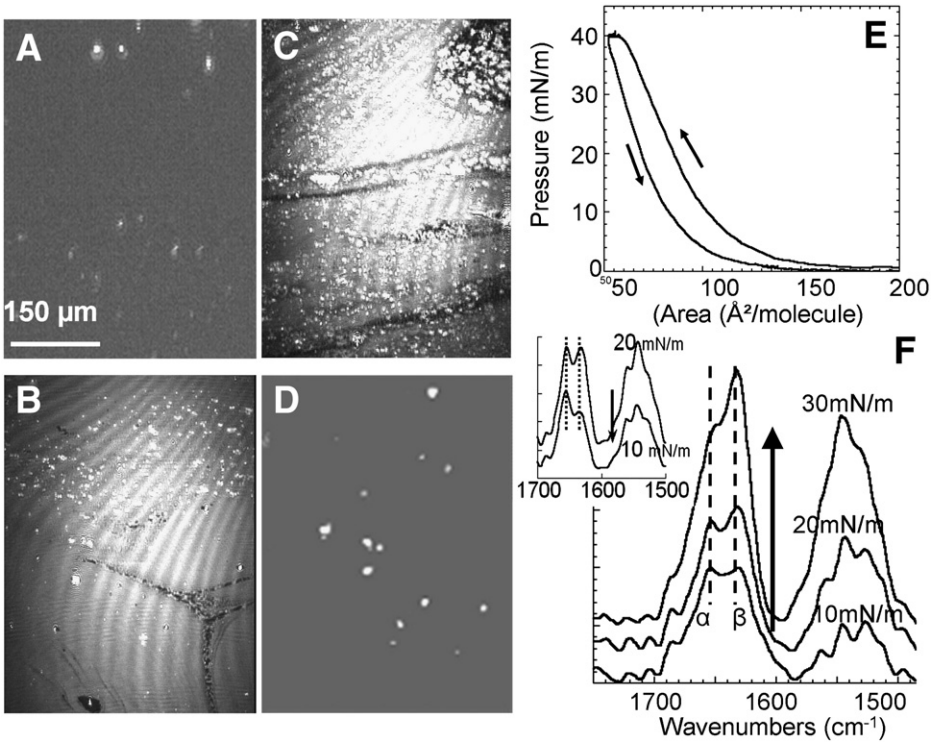

Fig. 1. Brewster angle microscopy of VAMP1. A)–D) BAM images of VAMP1 at the air–water interface in the absence of lipids, A) equilibrium at the surface pressure 0 mN/m ($R = 1.7\ e^{-7}$, ET = 20 ms, 7 Å); after protein film compression: B) at 20 mN/m ($R = 1.2\ e^{-6}$, ET = 20 ms, 30 Å), C) at 30 mN/m ($R = 1.34\ e^{-5}$, ET = 4 ms, 38 Å), and D) after total decompression (0 mN/m, $R = 5.7\ e^{-7}$, ET = 20 ms, 12 Å). E) Isotherm cycle of the VAMP1 at the buffer surface. Direction of the compression–decompression cycle is given by arrows. F) PMIRRAS spectra of VAMP1 at the buffer surface recorded at 10, 20 and 30 mN/m. The insert spectra are those during decompression to show the reversible transition. The spectra are shifted vertically for better visibility.

for proteins (see Materials and methods). Thus, most of the proteins probably spread over the air–water interface in an extended conformation without forming aggregates.

These poorly organized and loosely distributed monolayers of VAMP1 were then compressed in order to evaluate the effect of increasing molecular interaction on their aggregation behavior. Upon compression, the average luminosity of the BAM images and the surface pressure increased gradually until the surface pressure reached about 40 mN/m, a pressure at which the monolayer collapsed. The strong amphiphilicity of the proteins allowed them to remain at the water surface throughout the compression. The luminosity of BAM images and the thickness of the monolayer continued to increase homogeneously during compression. At a lateral pressure of 20 mN/m and 30 mN/m, the thickness of the protein film was about 30 Å (Fig. 1B) and 38 Å (Fig. 1C), respectively. Note that a lateral pressure of 30 mN/m corresponds to that expected in cellular membranes as deduced from various observations [17]. When the protein film was subsequently decompressed after the collapse point, surface luminosity progressively decreased indicative of a relatively fast reversible dynamic assembly/disassembly of the protein. This is further supported by the weak hysteresis on the compression/decompression isotherm of the protein (Fig. 1E).

The macroscopic information on the protein assembly at the water surface obtained by the BAM images and surface pressure isotherm was then compared with PMIRRAS spectra which provide information about the molecular structure. The PMIRRAS spectra measured during compression displayed large amide I bands between 1600 and 1700 cm^{-1} with two main maxima at 1630 cm^{-1} (accompanied sometimes with a small band at 1690 cm^{-1}) and at 1655 cm^{-1}, the characteristic IR bands of ß-sheets and α-helices, respectively, along with a large amide II band centered at 1535 cm^{-1} [18–21] Interestingly, the ratio of the two maxima of the amide I band evolved during the compression: beyond a surface pressure of 20 mN/m the intensity of the band at 1633 cm^{-1} increased with respect to the one at 1655 cm^{-1}. This indicates that β-sheets became the dominant structure at high surface pressure (Fig. 1F).

The evolution of PMIRRAS spectra showed that along with the protein structure, the orientation of the proteins changed with respect to the water surface during compression. As to the α-helices, a decrease in the amide I (1650 cm^{-1} α-helix)/amide II ratio upon compression showed that the helix axis at low surface pressure became more perpendicular to the interface [22] during compression in comparison to its initial orientation parallel to the interface. The combination of a weak amide I′ band at 1690 cm^{-1} with a strong amide I at 1630 cm^{-1} suggested that initially the anti-parallel ß-sheets also oriented mainly parallel to the interface at low surface pressure. Upon compression, the amide I′ band at 1690 cm^{-1} became negligible reflecting the transformation of anti-parallel ß-sheets to parallel ones at high surface pressure. During decompression, the amide I band at 1630 cm^{-1} decreased more rapidly than the band at 1655 cm^{-1}, recovering the original spectra at low surface pressure before compression in which the α-helix was the majority structure (insert in Fig. 1F)). These observations confirmed the reversible dynamics of VAMP1 as deduced from BAM images.

Thus when dispersed in water, VAMP1 formed films at the air–water interface due to their amphiphilicity. At low surface pressure, α-helices coexist with anti-parallel ß-sheets both oriented parallel to the interface. During compression, ß-sheets became the dominant structure along with the transformation from anti-parallel to parallel configuration and these sheets oriented perpendicular to the surface at high surface pressure.

The proteins structure was subsequently investigated in the presence of lipid monolayers in order to elucidate the effect of protein/lipid interactions on the properties of VAMP1 proteins.

3.2. VAMP1 in the presence of a neutral lipid monolayer (DMPC)

Our earlier study on the transmembrane domain of VAMP1 ($VAMP_{TM22}$) in lipid membranes showed that the structure of the TM peptide depended on the peptide/lipid ratios: at a low ratio, the peptides formed α-helix and at a high ratio they converted to β-sheet [7]. The critical peptide/lipid ratio for the transition was found to be around 1/75. Therefore, in the present study, the protein structure was studied at two different protein/lipid ratios, 1/83 and 1/33. Fig. 2 (A) compares the evolution of the BAM images of a DMPC monolayer either alone (a–c) or in the presence of VAMP1 at a ratio of 1/83 (d–f) and at different lateral pressures (0, 30 and 40 mN/m) at the surface of a phosphate buffer (pH 7.4). On the one hand, the DMPC monolayer alone displayed a quasi homogeneous liquid phase whose thickness increased uniformly with the compression. A few bright spots appeared that are characteristic of lipid aggregates, as previously reported (14 Å at 0 mN/m and 18 Å at 40 mN/m) [12].

On the other hand, the average luminosity of the mixed VAMP1/DMPC layer increased strongly at a surface pressure beyond 30 mN/m and segregations appeared between very small bright aggregates,

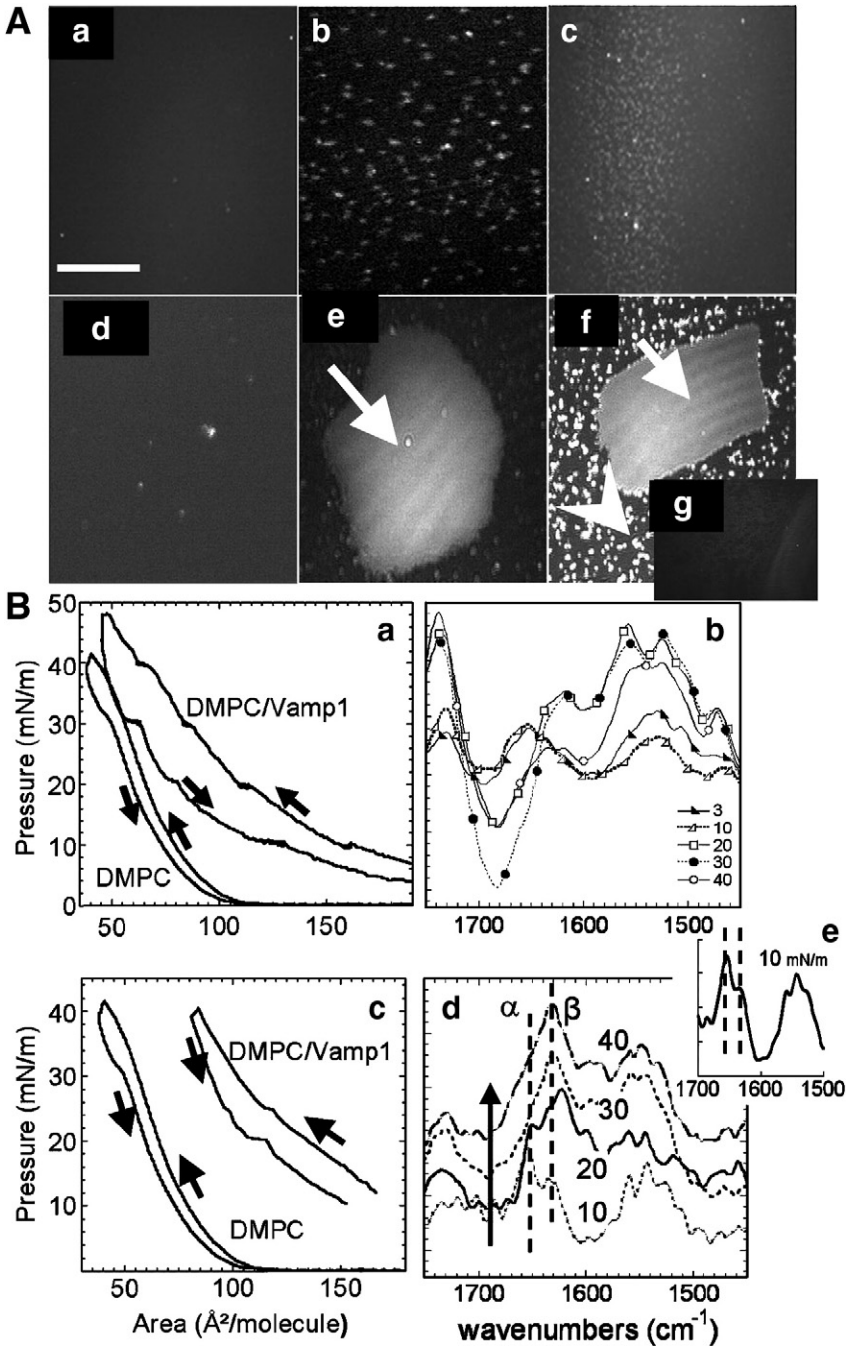

Fig. 2. A: BAM images of: DMPC layer a) at equilibrium on the interface (0 mN/m, GL = 37, $R = 9.5\ e^{-7}$, 14 Å); b) at 30 mN/m (GL = 45, $R = 1.5\ e^{-6}$, 18 Å); and c) at 40 mN/m (GL = 45, $R = 1.6\ e^{-6}$, 18 Å). Mixed 1/83 VAMP1/DMPC monolayer d) at 0 mN/m (GL = 42, $R = 1.2\ e^{-6}$, 14 Å); e) at 30 mN/m large bright domain (arrow) (GL = 85, $R = 2.6\ e^{-6}$, 22 Å); f) at 40 mN/m the appearance of large bright domain (arrow) (GL = 155, $R = 9.5\ e^{-6}$, 38 Å) and very bright small spots (arrow head) reflect highly condensed protein/lipid aggregates with higher thickness. Dark domains in both images (e, f) are 18 Å thick (GL = 90, $R = 1.4\ e^{-6}$). B: Isotherm cycles a) and PMIRRAS spectra recorded at 3, 10, 20, 30 and 40 mN/m b) of the DMPC monolayer and the mixed DMPC/VAMP1 monolayer 1/83 during compression. Isotherm cycles c) and PMIRRAS spectra recorded at 10, 20, 30 and 40 mN/m d) of the DMPC monolayer and the mixed DMPC/VAMP1 monolayer 1/33 during compression. The insert spectrum e) is taken after the surface pressure was decreased back to 10 mN/m. For d), the spectra are shifted vertically for better visibility.

larger homogeneous bright domains and dark domains. The large bright domains showed rigid rectangular shapes and their thickness was estimated as 42 Å at 40 mN/m corresponding to the typical thickness of a lipid bilayer (using an averaged refractive index of 1.465, considering $n=1.46$ for pure lipid and $n=1.47$ for VAMP1). Interestingly, the presence of these proteins induced the formation of lipid bilayers whereas they are usually not stable at water surface [23].

3.2.1. PMIRRAS spectra at a protein/lipid ratio of 1/83

Secondary protein structure was evaluated using PMIRRAS. A large amide II band between 1500 and 1600 cm^{-1} was apparent (Fig. 2(B)b) which became more prominent with increased surface pressure. For the amide I bands between 1600 and 1700 cm^{-1}, on the other hand, it changed the sign between low surface pressure (positive) and high surface pressure (negative). At low surface pressure up to 10 mN/m, a positive amide I band with its maximum at around 1652 cm^{-1} (dominant) characteristic of α-helices and a shoulder at around 1635 cm^{-1} characteristic of β-sheets were observed. As surface pressure exceeded ~20 mN/m, a negative band at 1680 cm^{-1} became dominant whilst keeping a positive band at 1630 cm^{-1} which increased with increasing surface pressure. The ensemble of these evolutions reflected a global orientation of α-helices and β-sheets from horizontal to vertical orientation upon the increase of the lateral pressure [14,23]. This is reminiscent to the results obtained with monolayers of VAMP1 in the absence of lipids (see above). This alteration of protein orientation may result from interactions between protein molecules brought into close contact upon compression. For the secondary structure of the protein, due to the change in the sign of the signal, it was not possible to evaluate the variation of the relative proportion of α-helices and β-sheets during compression. It seems that α-helices remain a dominant structure throughout the compression.

As it was observed for the monolayer of VAMP 1, the mixed DMPC/VAMP1 monolayer also showed a relatively fast reversible dynamics in the assembly/disassembly cycle of the protein during decompression: low hysteresis on the compression/decompression isotherm of the proteins (Fig. 2(B)a) and a reversible evolution of BAM images as well as of amide I and II bands were observed upon decompression.

3.2.2. The PMIRRAS spectra at a protein/lipid ratio of 1/33

Large and positive amide I bands between 1600 and 1700 cm^{-1} and a large amide II band centered at 1535 cm^{-1}1 were apparent (Fig. 2(B)d). At low surface pressure, the amide I band exhibited two maxima at 1655 cm^{-1} (dominant) and at 1630 cm^{-1} characteristic of α-helices and β-sheets, respectively. As the surface pressure exceeded ~20 mN/m, the initially predominant band at 1655 cm^{-1} diminished and the band at 1630 cm^{-1} increased, reflecting a global change of the protein structure from α-helices to β-sheets induced upon the increase of the lateral pressure. This is reminiscent to the results obtained with monolayers of VAMP1 in the absence of lipids (see above). This structural transition was concomitant to the appearance of bright domains in the BAM images at a surface pressure of 30 mN/m.

The change in the structure of VAMP1 was also accompanied by a change in its orientation in the lipid monolayer at the interface. During compression, the axis of the α-helix oriented almost parallel to the plane of the lipid monolayer at low surface pressure became more vertical in regard to the DMPC layer as the amide I (1650 cm^{-1})/amide II ratio decreased. Also the β-sheets present were oriented more vertically at higher surface pressure as shown by the increasing amide I (1630 cm^{-1})/amide II (1535 cm^{-1}). This alteration of protein orientation may result from interactions between protein molecules brought into close contact upon compression.

As it was observed for the monolayer of VAMP 1, the mixed DMPC/VAMP1 monolayer also showed relatively fast reversible dynamics in the assembly/disassembly cycle of the protein during decompression: a low hysteresis on the compression/decompression isotherm of the proteins (Fig. 2(B)a), and a reversible evolution of BAM images (Fig. 2(A)g) as well as of amide I band ratios (1630 cm^{-1}/1655 cm^{-1}), indicative for the recovery of an α-helical structure upon decompression (Fig. 2(B)e).

3.3. VAMP1 and DMPG monolayer: anionic lipid layer (protein peptide/lipid ratio of 1/83)

According to Takamori et al. [24], the ratio of various lipids on synaptic vesicles amounts to 24% phosphatidylcholine (PC), 15% phosphatidylethanolamine (PE), 8% phosphatidylserine (PS) and 53% cholesterol (Chol) where PS represents charged (anionic) lipids. As PS interferes with the PMIRRAS signals of the amide bands, we have used another negatively charged lipid, i.e. DMPG, in order to investigate charge effects on the structure of VAMP1. Fig. 3 shows BAM images of a pure DMPG monolayer compared with a DMPG monolayer in the presence of VAMP1 (protein/lipid ratio of 1/83) at different lateral pressures during surface compression. The surface compression isotherm and PMIRRAS spectra of the amide bands of VAMP1 are also provided.

An important difference was observed between the BAM images of the DMPG and DMPC monolayers. At low surface pressure, a homogeneous monolayer of DMPG in its expanded liquid phase was present. Increases in surface pressure were accompanied by lipid phase transition [25] at around 18 mN/m from an expanded liquid phase (dark domains, thickness ~9 Å) to a condensed liquid phase (bright domains, thickness ~18 Å). Upon further compression, bright lipid domains became dominant. At a pressure of 25 mN/m, they covered the entire surface and their thickness was estimated to be about 20 Å (using a refractive index of 1.46) as expected for a condensed DMPG monolayer.

In the presence of VAMP1, the BAM image at low pressure demonstrated coexistence of expanded liquid phase lipid monolayers with protein aggregates as bright spots. Interestingly, at higher pressure, these aggregates coalesced and a homogeneous protein/DMPG monolayer of ~28 Å thickness was observed. This behavior is in stark contrast to the VAMP1/DMPC system in which segregation between protein-rich and -poor regions was observed upon compression.

The broad amide I band of VAMP1 in DMPG layer observed in PMIRRAS spectra represented a mixture of α-helices, representing the majority of structures, β-turns and anti-parallel β-sheets (bands centered at 1655 cm^{-1} with two shoulders around 1675 cm^{-1} and 1630 cm^{-1} coupled to a smaller band at 1685 cm^{-1}). Unlike the results obtained with DMPC monolayers, the proteins did not undergo a clear structural transition upon compression but retained mainly an α-helical structure. However, the global amide I band intensity did not increase upon compression and there was a clear decrease in the ratio of the amide I (1655 cm^{-1})/amide II bands (1535 cm^{-1}). This observation is compatible with the orientation of these α-helices evolving under compression from an almost parallel orientation to the interface at low pressure to a more perpendicular orientation to the interface at higher pressure.

VAMP1 has a positively charged juxtamembrane domain with 6 positively charged amino acids out of 12 at pH 7.4 (5 lysines and 1 arginine). Electrostatic interplay between negatively charged DMPG and VAMP1 might prohibit the formation of protein aggregates and induce the vertical orientation. The homogeneous BAM images during surface compression suggest that indeed non-aggregated proteins were homogeneously distributed within the lipid layer. During decompression from 45 mN/m to 10 mN/m, very little hysteresis was detected on the isotherm, again indicating the dynamic nature of the protein structure.

To further investigate the potential role of the lipid charge density of the membrane, we have chosen two different DMPC/DMPG ratios.

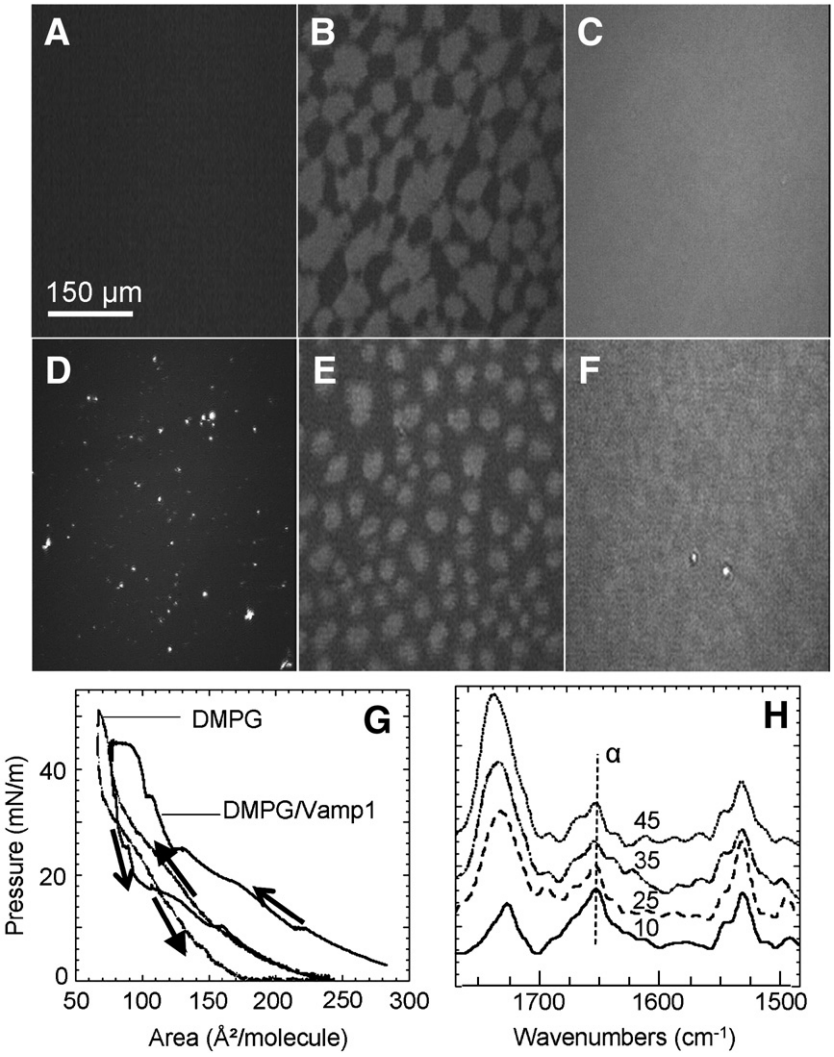

Fig. 3. A)–C) BAM images of a pure DMPG monolayer at different lateral pressures A) 0 mM/m ($R = 7.5\ e^{-7}$, 12 Å), B) 25 mM/m ($R = 1.7\ e^{-6}$, 18 Å), and C) 45 mM/m ($R = 2.8\ e^{-6}$, 20 Å) during surface compression. D)–G) BAM images of DMPG monolayer in the presence of VAMP1 D) 0 mM/m ($R = 1.5\ e^{-6}$, 17 Å), E) 25 mM/m ($R = 4.5\ e^{-6}$, 24 Å), F) 45 mM/m ($R = 6.2\ e^{-6}$, 28 Å). G) Isotherm cycles of the DMPG monolayer and the mixed DMPG/VAMP1 monolayer at the buffer surface during compression. H) PMIRRAS spectra of VAMP1 incorporated in a DMPG monolayer and recorded at 10, 25, 35 and 45 mN/m. The spectra are shifted vertically for better visibility.

Using a ratio of 2.3/1 similar to the PC to PS ratio found in synaptic vesicles [24], we focused on the ratio of PC to PS. In contrast, a 9/1 ratio approaches the ratio between the sum of all the neutral and zwitterionic lipids versus PS present in synaptic vesicles. In the latter case, we focused mainly on the lipid charge distribution.

3.4. VAMP1 in mixed lipid monolayer of 2.3/1 DMPC/DMPG (protein peptide/lipid ratio of 1/83)

Fig. 4 shows BAM images of the DMPC/DMPG (2.3/1) monolayer film in the absence or presence of VAMP1 along with surface compression isotherms and PMIRRAS spectra of the protein collected at different lateral pressure.

BAM images of DMPC/DMPG (2.3/1) films with or without VAMP1 at the surface exhibited a similar evolution to that observed with DMPG molecules alone at the interface. A phase transition from expanded liquid phase to condensed liquid phase (phase transition around 26 mN/m) was observed as seen by the formation of bright lipid patches at the surface. In the presence of VAMP1, the BAM images showed protein aggregates at low surface pressure. Upon compression, these domains disappeared and a homogeneous mixture of a 27 Å thick protein/lipid monolayer was observed, comparable to the DMPG/protein system.

PMIRRAS spectra were also similar to those of the DMPG/protein system; a large unresolved amide I band between 1600 and 1700 cm^{-1} centered at around 1655 cm^{-1} with small shoulders at around 1675 cm^{-1} and 1630 cm^{-1} and a small amide II band at 1535 cm^{-1}. No clear evidence of structural transition was observed throughout compression. The main difference to the pure DMPG system was a gradual change in protein orientation upon compression. The amide I/amide II ratio increased during the compression (Fig. 4: 1.97 for 20 mN/m to 7.45 for 47 mN/m) in contrast to the DMPG system. Whilst it is not possible to quantify the orientation of each secondary structure component, due to the coexistence of several structures as seen from large amide I band, some evidence is provided by the very weak intensity of the amide II band which furthermore decreased with compression. This observation indicates that the contribution of components from each structure should also be very weak and decrease with increasing surface pressure. Even though other components coexist as observed from the amide I band, the α-helical structure is the major one. Moreover, for these α-helical domains, the ratio of amide I/amide II does increase at high surface pressure, as the contribution of amide II approaches zero. Therefore, α-helical domains lie essentially parallel to the surface at high surface pressure.

Note that more than 80% of the full-length VAMP1 consists of the cytosolic and juxtamembrane domains and both contribute to the signal if the sequence is structured. Under these circumstances they

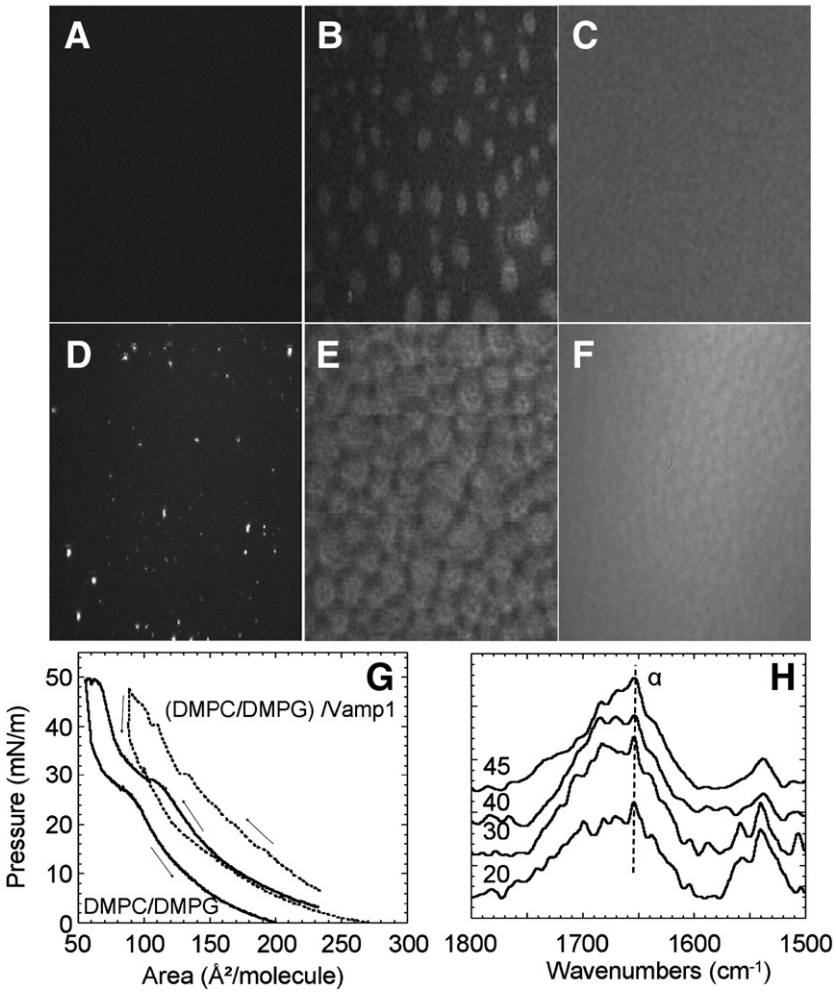

Fig. 4. A)–C) BAM images of a pure DMPC/DMPG (2/1) monolayer are shown at different lateral pressures A) 0 mM/m ($R=5.5\ e^{-7}$, 10 Å), B) 25 mM/m ($R=1.5\ e^{-6}$, 14 Å), and C) 45 mN/m ($R=2.7\ e^{-6}$, 20 Å) during surface compression. D)–F) BAM images of a DMPC/DMPG monolayer in the presence of VAMP1 d) 0 mM/m ($R=1.6\ e^{-6}$, 14 Å), E) 25 mM/m ($R=4.5\ e^{-6}$, 24 Å), and F) 45 mN/m ($R=6.9\ e^{-6}$, 29 Å). G) Isotherm cycles of the DMPC/DMPG monolayer and the mixed DMPC/DMPG/VAMP1 monolayer at the buffer surface during compression. H) PMIRRAS spectra of the DMPC/DMPG monolayer with VAMP1 incorporated and recorded at 20, 30, 40 or 45 mN/m. The spectra are shifted vertically for better visibility.

will provide the majority of the signal. Moreover, the highly hydrophobic transmembrane domains are surrounded by lipids and are thus not likely to lie parallel to the surface at high surface pressure. It is therefore most probable that the observed orientation reflects mainly the juxtamembrane and cytosolic domains that interact with the membrane surface.

3.5. VAMP1 in mixed lipid monolayer of 9/1 DMPC/DMPG (protein peptide/lipid ratio of 1/83)

The lipid mixture with a smaller DMPG ratio (DMPC/DMPG 9/1) displayed a broad amide I band in PMIRRAS spectra up to a pressure of 20 mM/m again centered at 1655 (α-helix), 1670 cm^{-1} (ß-turn) and at around 1645 and 1600 cm^{-1} (random structure) (Fig. 5). This may reflect the random structure of cytosolic domains [26,27] along with more structured membrane domains that are mainly α-helical. However, at higher surface pressures structural transformation differed from the one observed when using DMPC/DMPG at a 2.3/1 ratio. At 30 mN/m, the peak at 1630 cm^{-1} became dominant and was accompanied by a peak at 1690 cm^{-1}. Clearly, protein structures transformed in majority to β-sheets upon compression and at least a part of them were oriented in anti-parallel fashion. This observation on the role of protein/lipid density on the increased presence of β-sheet is further corroborated by our observation on VAMP1 inserted into monodisperse unilamellar vesicles (see Fig. S1). Importantly, the amide I (1630 cm^{-1})/amide II ratio in PMIRRAS spectra in the DMPC/DMPG 9/1 system decreased during the compression, clearly indicating that anti-parallel β-sheets were oriented with the peptide chains parallel to the water–lipid interface at higher surface pressure. Although PMIRRAS spectra do not allow discrimination of transmembrane domains from cytosolic parts, these anti-parallel β-sheets are unlikely to represent membrane domains of the protein for several reasons. As previously reported by us [7] and others [28], tilted β-sheets destabilize membranes, whereas we did not observe such an effect on vesicle membranes (see supporting information in Fig. S1, where stable vesicles were observed). In addition, the authors previously observed in another model system that the β-sheets formed by transmembrane domains became more perpendicular to the monolayer as the surface pressure was increased even when initially they formed parallel β-sheets which lie parallel with the monolayers at low surface pressure [16]. This transformation from anti-parallel β-sheets to parallel β-sheets accompanied by the change in their orientation is most likely due to steric reasons [16]. In the present case, it is probably the strong cationic character of the juxtamembrane domain (6 amongst 12 amino acids are cationic with no anionic ones for the first 16 amino acids) which induces its organization parallel to the negatively charged monolayer interface. The transmembrane domain will probably remain in α-helical

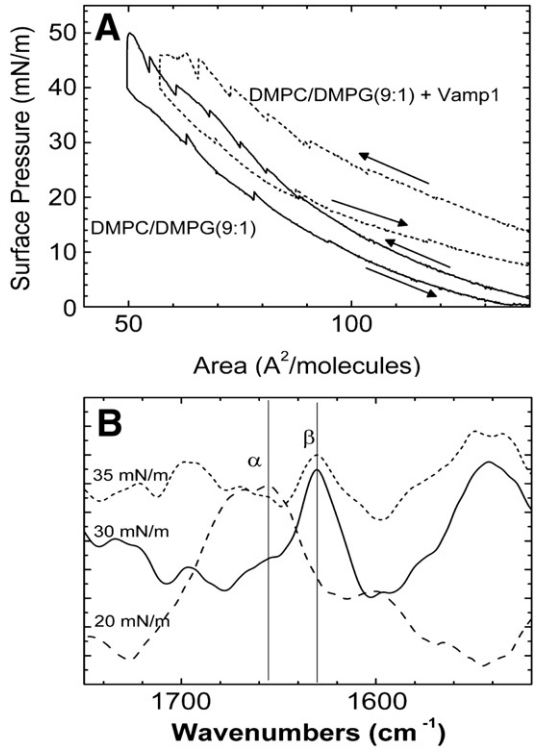

Fig. 5. A) Isotherm cycles of the DMPC/DMPG monolayer (9:1) and the mixed DMPC/DMPG/VAMP1 monolayer at the buffer surface during compression. B) PMIRRAS spectra of VAMP1 incorporated in the DMPC/DMPG monolayer (9:1) and recorded at 20, 30 and 35 mN/m. The PMIRRAS spectra are shifted vertically for better visibility.

configuration. Since they are incorporated in lipid monolayers, these α-helices are oriented in a direction such that the corresponding amide I band is very weak (~45°) and this may explain the relatively small amplitude of the amide I band observed here.

Thus, whilst the structural transition from α-helices to β-sheets upon compression is similar to that observed in the presence of DMPC monolayer, the major difference at a DMPC/DMPG ratio of 9/1 is given by the formation of anti-parallel β-sheets and their orientation with respect to the interface at high surface pressure. Indeed, in DMPC monolayers VAMP1 formed parallel β-sheets which were oriented perpendicular to the interface. Again, the interaction of cationic juxtamembrane domains of the proteins with anionic lipid head groups probably provides the driving force for protein organization and orientation parallel to the interface at increased surface pressure.

The result of deconvolution of the PMIRRAS spectra is summarized in Table 1. The increase in β-sheet structures with respect to α-helical structures during compression is clearly observed for monolayers containing only VAMP as well as for VAMP in the presence of DMPC lipid layer. In the presence of DMPG or DMPC/DMPG (3/1) lipid layers VAMP1 remains mainly as α-helical structure throughout the compression. In these cases, the ratio between Amide I and Amide II bands unambiguously showed the evolution of the protein orientation with respect to the lipid monolayer. The increase of the amide I/amide II ratio (in the case of VAMP in the presence of DMPC/DMPG lipid layer) demonstrated that α-helices became more horizontally oriented at high surface pressure, whereas a decrease of the ratio (in the case of VAMP in the presence of DMPG lipid layer) during compression was observed as the α-helices were oriented vertically with the lipid layers.

4. Discussion

We have investigated the behavior of a full-length transmembrane protein and collectively the data obtained reveal the importance of protein–lipid interaction and the considerable sensitivity of VAMP1 in lipid layers to its environment in terms of structure and orientation. A schematic summary is represented in the Fig. 6.

Three factors are particularly important for protein structures, for protein orientation with respect to lipid monolayer and for protein–protein interaction: lateral pressure of the monolayers, protein/lipid ratio and the surface charge density of the lipid layer. These three parameters are physiologically present and regulated in cellular membranes. Their influence is shown for example in the BAM images of protein/DMPC films which demonstrated segregation between thick and thin domains upon compression at high pressure. In contrast, this segregation was absent in BAM images of the protein/DMPG system. The strong interaction between the negative charges on the polar heads of DMPG and positive charges provided by the soluble (cytosolic) residues of the proteins seems to stabilize uniformly mixed bilayers on the Langmuir trough under compression.

Table 1
The results of deconvolution of the PMIRRAS spectra for various secondary structures of VAMP proteins. Deconvolution was performed with four different structures; α-helix (~1655 cm^{-1}), β-sheet (~1620–1630 cm^{-1}), random (~1640 cm^{-1}), and β-turn (~1670 cm^{-1}) and the absolute values are given. For VAMP protein monolayer and VAMP in DMPC (VAMP/DMPC 1/33) the ratio of α-helix and β-sheet structures evolved clearly during compression. For the systems in which the secondary structure did not change during the compression and remained α-helical such as VAMP in DMPC/DMPG (1/2.3) or VAMP in DMPG, $\sum Amide\ I / \sum Amide\ II$ gave the indication of the orientation of α-helices with respect to the air–water surface during compression.

	α-helix	β-sheets	β/α	Random	β-turn	$\sum Amide\ I / \sum Amide\ II$	Correlation factor
VAMP (mN/m)							
10	0.03	0.03	**1.231**	0.03	0.004	2.29	1.016
20	0.03	0.05	**1.500**	0.04	0.004	1.29	1.042
40	0.04	0.09	**2.143**	0.05	0.008	1.15	1.014
VAMP in DMPC (1/33) (mN/m)							
10	0.07	0.01	**0.192**	0.005	0.002	*1.30*	*1.000*
20	0.04	0.05	**1.184**	0.003	0.02	*3.37*	*1.000*
30	0.03	0.06	**2.370**	0.002	0.01	*1.03*	*0.994*
40	0.03	0.08	**2.600**	0.009	0.01	*1.50*	
VAMP in DMPC/DMPG (1/2.3) (mN/m)							
20	0.03	0.02	0.529	0.005	0.03	**1.97**	0.995
30	0.04	0.02	0.487	0.04	0.02	**3.52**	1.000
40	0.04	0.02	0.436	0.04	0.007	**6.87**	0.991
47	0.05	0.02	0.429	0.02	0.02	**7.45**	1.001
VAMP in DMPG (mN/m)							
10	0.02	0.003	0.132	0.006	0.007	**1.98**	1.054
25	0.01	0.005	0.343	0.003	0.01	**1.29**	1.069
35	0.02	0.005	0.242	0.01	0.005	**1.17**	1.035
45	0.01	0.003	0.343	0.003	0.01	**0.89**	1.015

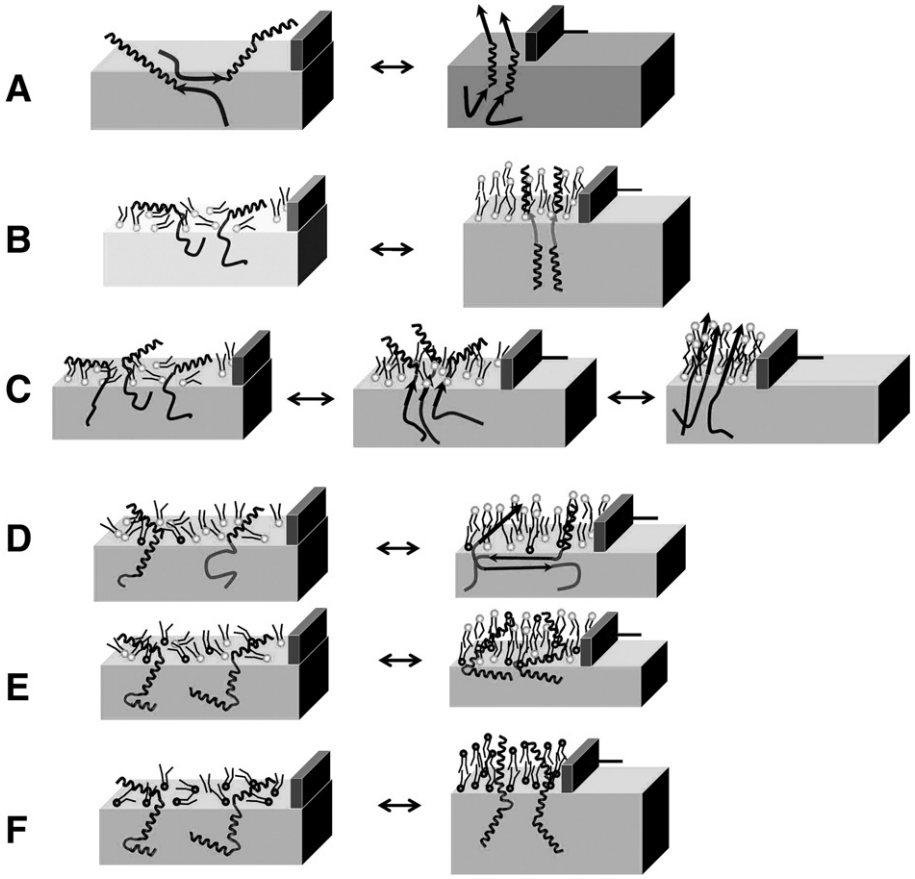

Fig. 6. Schematic representation of the dynamic structure of VAMP1 at an air/water interface upon compression with various lipid compositions. A) In the absence of lipids, α-helices convert to parallel β-sheets upon compression, B) in the presence of DMPC, with the protein to lipid ratio of 1/83, the structure of VAMP1 remain α-helical in majority all through compression, but they get strongly aligned perpendicular to air–water interface at high surface pressure. C) At higher protein to lipid ratio; 1/33, conversion from α-helices to parallel β-sheets occurs as in a). D) In the presence of DMPC/DMPG (9/1 mixture) conversion occurs, however the presence of anti-parallel β-sheets which lie flat at the interface is observed upon compression, E) using a more negatively charged lipid monolayer, DMPC/DMPG (2.3/1 mixture), the compression is accompanied mainly by changes in orientation and organization at the interface of α-helices which become aligned with interface at higher surface pressure, and F) in the presence of pure DMPG monolayer, VAMP1 remains α-helical during the compression, but becomes vertical to the interface at high surface pressure.

From a structural point of view, at low protein/lipid ratio and/or at low surface pressure condition, VAMP1 adopted predominantly α-helical secondary structure with some β-turns regardless of the surrounding lipid. Upon compression, a reversible transition from α-helical to β-sheet structure was observed for the protein monolayer. Transition was also observed in the presence of the neutral DMPC layer at high protein to lipid ratio (Figs. 2 and 6C). As the charge density of the lipid layer was modified by addition of negatively charged lipids such as DMPG, structural transition was observed up to a charge density of 10 mol% (Fig. 6D), which corresponds to the surface charge density reported for synaptic vesicles [24]. Beyond 30 mol% of DMPG, transition did not occur and the protein remained α-helical throughout the compression (Fig. 6e and f). This underlines the importance of lipid–protein interactions as a major factor on protein organization in the lipid membrane.

One may question the validity of the use of supported lipid mono/bilayers at an air–water interface as a model membrane system. However, these results are in good agreement with our previous findings on the structure of the transmembrane domain of VAMP 1 in the presence of neutral lipids, DOPC or DMPC [7] performed in different model systems such as multibilayer system, unilamellar vesicles, as well as the Langmuir film. These studies underlined the same tendency: at lower peptide to lipid ratio, the secondary structure of the TMD peptides remained α-helical whereas at higher ratio, a reversible transition to β-sheets was observed. The structural properties of VAMP1 in the presence of DMPC monolayers (at 1/83 and at 1/33 ratio) reported now agree very well with this behavior. In the present study, the presence of juxtamembrane and cytosolic domains renders VAMP1 sensitive to charges of lipid headgroups. Moreover, the structural investigation of full-length VAMP1 inserted into unilamellar vesicles was performed using circular dichroism as a function of different peptide/lipid ratios at a fixed negative phospholipid ratio (80% DOPC/20% DOPS) (Supporting information). Again, the transition between α-helical and β-sheet conformations was observed upon increasing protein to lipid ratios illustrating the sensitivity of the secondary structure of VAMP1 to lipid charge density of vesicle membranes along with the surface pressure.

In all four lipid systems reported in this study, the compression was accompanied by important changes in the orientation of the protein at/in the lipid film. In pure (neutral) DMPC or pure (charged) DMPG systems (Fig. 6B, C and F) the orientation of proteins became more perpendicular to the membrane surfaces at high surface pressure. In contrast, with a DMPC/DMPG lipid mixture, juxtamembrane domains of the protein were observed to lie flat at the lipid membrane surface at high surface pressure (Fig. 6C and D) regardless of the protein conformation. This clearly demonstrates that the variation of the negative charge density of the lipid film has an important effect on the protein orientation most likely through strong interactions with the juxtamembrane domain of the proteins. Matching the density of lipid charges and protein charges may be the key factor which controls the protein orientation in relation to the membrane surface. Interestingly, structural transitions of the transmembrane domain depend on peptide/lipid ratios, whereas the transition of the cytosolic portions of the protein depends on the surface

charge (Fig. 6D vs. E). It is noteworthy that all the structural and orientational changes observed upon compression were reversible regardless of the lipid, indicating the dynamic behavior of the protein. Obviously care has to be applied, however, when drawing conclusions about the situation in biological systems. The presence of numerous other transmembrane proteins as well as the dynamic recruitment of cytosolic proteins to the membrane surface and to SNARE proteins [3,24] may alter the charge density acting on VAMP1. It is, however, intriguing to speculate that the highly dynamic structure of VAMP may have physiological relevance as both protein density and phospholipid charges are known to be regulated during membrane fusion [29–31].

Acknowledgements

This work was supported by funds from the ACI (DRAB), the Université de Bordeaux 1 (BQR), the Agence National de Recherche (ANR) and the Fondation de Recherche Médicale (FRM).

Appendix A. Supplementary data

Supplementary data associated with this article can be found, in the online version, at doi:10.1016/j.bbamem.2010.01.009.

References

[1] A. Mayer, Membrane fusion in eukaryotic cells, Annu. Rev. Cell Dev. Biol. 18 (2002) 289–314.
[2] A.T. Brunger, K. Weninger, M. Bowen, S. Chu, Single-molecule studies of the neuronal SNARE fusion machinery, Annu. Rev. Biochem. 78 (2009) 903–928.
[3] T.C. Sudhof, J.E. Rothman, Membrane fusion: grappling with SNARE and SM proteins, Science 323 (2009) 474–477.
[4] T. Sollner, S.W. Whiteheart, M. Brunner, H. Erdjument-Bromage, S. Geromanos, P. Tempst, J.E. Rothman, SNAP receptors implicated in vesicle targeting and fusion, Nature 362 (1993) 318–324.
[5] T. Weber, B.V. Zemelman, J.A. McNew, B. Westermann, M. Gmachl, F. Parlati, T.H. Sollner, J.E. Rothman, SNAREpins: minimal machinery for membrane fusion, Cell 92 (1998) 759–772.
[6] J. Rizo, X. Chen, D. Arac, Unraveling the mechanisms of synaptotagmin and SNARE function in neurotransmitter release, Trends Cell Biol. 16 (2006) 339–350.
[7] W. Yassine, N. Taib, S. Federman, A. Milochau, S. Castano, W. Sbi, C. Manigand, M. Laguerre, B. Desbat, R. Oda, J. Lang, Reversible transition between α-helix and β-sheet conformation of a transmembrane domain, Biochim. Biophys. Acta - Biomembranes 1788 (2009) 1722–1730.
[8] F. Boal, H. Zhang, C. Tessier, P. Scotti, J. Lang, The variable C-terminus of cysteine string proteins modulates exocytosis and protein–protein interactions, Biochemistry 43 (2004) 16212–16223.
[9] C. Monterrat, F. Boal, F. Grise, A. Hemar, J. Lang, Synaptotagmin 8 is expressed both as a calcium-insensitive soluble and membrane protein in neurons, neuroendocrine and endocrine cells, Biochim. Biophys. Acta - Mol. Cell Biol. 1763 (2006) 73–81.
[10] S.J. Johnson, T.M. Bayerl, W. Weihan, H. Noack, J. Penfold, R.K. Thomas, D. Kanellas, A.R. Rennie, E. Sackmann, Coupling of spectrin and polylysine to phospholipid monolayers studied by specular reflection of neutrons, Biophys. J. 60 (1991) 1017–1025.
[11] S. Castano, B. Delord, A. Fevrier, J.M. Lehn, P. Lehn, B. Desbat, Brewster angle microscopy and PMIRRAS study of DNA interactions with BGTC, a cationic lipid used for gene transfer, Langmuir 24 (2008) 9598–9606.
[12] J. Saccani, S. Castano, F. Beaurain, M. Laguerre, B. Desbat, Stabilization of phospholipid multilayers at the air–water interface by compression beyond the collapse: a BAM, PM-IRRAS, and molecular dynamics study, Langmuir 20 (2004) 9190–9197.
[13] V.P. Tolstoy, I.V. Chernyshova, V.A. Skryshevsky, Handbook of Infrared Spectroscopy of Ultrathin Films, Wiley, Hoboken, NJ, USA, 2003.
[14] D. Blaudez, J.M. Turlet, J. Dufourcq, D. Bard, T. Buffeteau, B. Desbat, Investigation at the air/water interface using polarization modulation IR spectroscopy, J. Chem. Soc. Faraday Trans. 92 (1996) 525–530.
[15] L. Mao, A.M. Ritcey, B. Desbat, Evaluation of molecular orientation in a polymeric monolayer at the air/water interface by polarization-modulated infrared spectroscopy, Langmuir 12 (1996) 4754–4759.
[16] I. Vergne, B. Desbat, Influence of the glycopeptidic moiety of mycobacterial glycopeptidolipids on their lateral organization in phospholipid monolayers, Biochim. Biophys. Acta 1467 (2000) 113–123.
[17] D. Marsh, Lateral pressure profile, spontaneous curvature frustration, and the incorporation and conformation of proteins in membranes, Biophys. J. 93 (2007) 3884–3899.
[18] P.I. Haris, D. Chapman, Does Fourier-transform infrared spectroscopy provide useful information on protein structures? Trends Biochem. Sci. 17 (1992) 328–333.
[19] T. Miyazawa, E.R. Blout, The infrared spectra of polypeptides in various conformations: amide I and II bands, J. Am. Chem. Soc. 83 (1961) 712–719.
[20] W.H. Moore, S. Krimm, Vibrational analysis of peptides, polypeptides, and proteins. II. beta-poly(L-alanine) and beta-poly(L-alanylglycine), Biopolymers 15 (1976) 2465–2483.
[21] W.K. Surewicz, H.H. Mantsch, D. Chapman, Determination of protein secondary structure by Fourier transform infrared spectroscopy: a critical assessment, Biochemistry 32 (1993) 389–394.
[22] I. Cornut, B. Desbat, J.M. Turlet, J. Dufourcq, In situ study by polarization modulated Fourier transform infrared spectroscopy of the structure and orientation of lipids and amphipathic peptides at the air–water interface, Biophys. J. 70 (1996) 305–312.
[23] P. Na Nakorn, M.C. Meyer, C.R. Flach, R. Mendelsohn, H.J. Galla, Surfactant protein C and lung function: new insights into the role of alpha-helical length and palmitoylation, Eur. Biophys. J. 36 (2007) 477–489.
[24] S. Takamori, M. Holt, K. Stenius, E.A. Lemke, M. Gronborg, D. Riedel, H. Urlaub, S. Schenck, B. Brugger, P. Ringler, S.A. Muller, B. Rammner, F. Grater, J.S. Hub, B.L. De Groot, G. Mieskes, Y. Moriyama, J. Klingauf, H. Grubmuller, J. Heuser, F. Wieland, R. Jahn, Molecular anatomy of a trafficking organelle, Cell 127 (2006) 831–846.
[25] C. Mombers, J. de Gier, R.A. Demel, L.L. van Deenen, Spectrin–phospholipid interaction. A monolayer study, Biochim. Biophys. Acta 603 (1980) 52–62.
[26] D. Fasshauer, H. Otto, W.K. Eliason, R. Jahn, A.T. Brunger, Structural changes are associated with soluble N-ethylmaleimide-sensitive fusion protein attachment protein receptor complex formation, J. Biol. Chem. 272 (1997) 28036–28041.
[27] M. Margittai, D. Fasshauer, S. Pabst, R. Jahn, R. Langen, Homo- and heterooligomeric SNARE complexes studied by site-directed spin labeling, J. Biol. Chem. 276 (2001) 13169–13177.
[28] M. Bowen, A.T. Brunger, Conformation of the synaptobrevin transmembrane domain, Proc. Nat'l Acad. Sci. U. S. A. 103 (2006) 8378–8383.
[29] G. Di Paolo, P. De Camilli, Phosphoinositides in cell regulation and membrane dynamics, Nature 443 (2006) 651–657.
[30] J.C. Hay, P.L. Fisette, G.H. Jenkins, K. Fukami, T. Takenawa, R.A. Anderson, T.F. Martin, ATP-dependent inositide phosphorylation required for Ca^{2+}-activated secretion, Nature 374 (1995) 173–177.
[31] J. Lang, PIPs and pools in insulin secretion, Trends Endocrinol. Metab. 14 (2003) 297–299.